Steering of a Sub-GeV Electron Beam through Planar Channeling Enhanced by Rechanneling

A. Mazzolari, E. Bagli, L. Bandiera, and V. Guidi*
INFN Sezione di Ferrara, Dipartimento di Fisica e Scienze della Terra, Università di Ferrara Via Saragat 1, 44100 Ferrara, Italy

H. Backe and W. Lauth
Institut für Kernphysik der Universität Mainz, Fachbereich Physik, Mathematik und Informatik, D-55099 Mainz, Germany

V. Tikhomirov
Research Institute for Nuclear Problems, Belarusian State University, Bobruiskaya street, 11, Minsk 220030, Belarus

A. Berra, D. Lietti, and M. Prest
Università dell'Insubria, via Valleggio 11, 22100 Como, Italy and INFN Sezione di Milano Bicocca, Piazza della Scienza 3, 20126 Milano, Italy

E. Vallazza
INFN Sezione di Trieste, Via Valerio 2, 34127 Trieste, Italy

D. De Salvador
INFN Laboratori Nazionali di Legnaro, Viale dell'Università 2, 35020 Legnaro, Italy and Dipartimento di Fisica, Università di Padova, Via Marzolo 8, 35131 Padova, Italy

(Received 2 December 2013; published 2 April 2014)

We report the observation of efficient steering of a 855 MeV electron beam at MAMI (MAinzer MIkrotron) facilities by means of planar channeling and volume reflection in a bent silicon crystal. A 30.5 μm thick plate of (211) oriented Si was bent to cause quasimosaic deformation of the (111) crystallographic planes, which were used for coherent interaction with the electron beam. The experimental results are analogous to those recorded some years ago at energy higher than 100 GeV, which is the only comparable study to date. Monte Carlo simulations demonstrated that rechanneling plays a considerable role in a particle's dynamics and hinders the spoiling of channeled particles. These results allow a better understanding of the dynamics of electrons subject to coherent interactions in a bent silicon crystal in the sub-GeV energy range, which is relevant for realization of innovative x-ray sources based on channeling in periodically bent crystals.

DOI: 10.1103/PhysRevLett.112.135503 PACS numbers: 61.85.+p, 29.27.-a

Since the seminal work of Tsyganov (1976) [1], beam manipulation assisted by bent crystals has been demonstrated to be a powerful tool to steer positively charged particle beams [2]. Three coherent interaction mechanisms, i.e., planar channeling [3–5], axial channeling [6], and volume reflection (VR) [7,8], provide relevant opportunities in terms of steering efficiency and ease of implementation in existing accelerators. To date, crystal-assisted beam steering has been extensively investigated for positively charged particle beams, spanning from MeV [9] to GeV [10,11] and TeV energies [12–14]. The use of bent crystals has also been suggested to collimate the beam in the Large Hadron Collider (LHC) [15] and realize a 7 TeV-extracted beam line for the LHC [16,17].

In contrast, steering of a negatively charged particle beam via coherent interactions in bent crystals is still at its infancy. Despite that, relevant applications have been suggested over a wide range of energies. On the very high-energy side, crystal-aided collimation was proposed for beam collimation of the International Linear Collider [18], while in the GeV energy range, which is accessible by most electron accelerators worldwide, beam steering in periodically bent crystals is interesting for the realization of innovative high-intensity radiation sources [19–21]. Achievement of such goals does demand greater knowledge on coherent interactions for negative particles. Previous experiments attempting the steering of negative-particle beams through bent crystals were unsuccessful [22,23] because crystals with length much larger than the dechanneling length were used. In such cases, channeled particles were scattered out of the crystal and no particle arrived at the angle of the nominal deflection of the crystal.

Only recently, experiments performed with 150 GeV negative pions [24–27] demonstrated that a crystal with a length comparable with the dechanneling length (about 1 mm at that energy) allowed the achievement of channeling up to the nominal bending of the crystal, and VR as for their positively charged counterparts [6,8,28].

In the GeV energy range, steering of negatively charged particles through bent crystals has never been reported mostly because of the difficulties to fabricate a bent crystal featuring a short thickness along the beam. Indeed, pioneering experiments with straight crystals [29,30] provided a measurement of the dechanneling length of GeV electrons channeled between (110) silicon planes, which turned out to be in the range of a few tens of microns.

In this Letter, we report about efficient steering of a sub-GeV electron beam by means of planar channeling and VR. A Monte Carlo simulation was carried out, highlighting that particle rechanneling plays a crucial role in obtaining high deflection efficiency for channeling; i.e., a significant fraction of particles subject to dechanneling is rechanneled and contributes to the deflection efficiency.

A proposal for a silicon crystal optimized for steering of GeV electrons was recently suggested in Ref. [31]. It consists of a platelike crystal with short thickness along the beam, which is bent through the quasimosaic effect [32] [see Fig. 1(a)]. The crystallographic orientations were chosen in order to obtain bending of (111) planes, which were used for deflecting the electron beam. Thus, a silicon crystal 30.5 ± 0.5 μm thick, with crystallographic orientations as in Fig. 1(a), was fabricated by starting with a 500 μm thick (211) Si wafer. The wafer was diced to thin plate crystals through a revisitation of the so-called

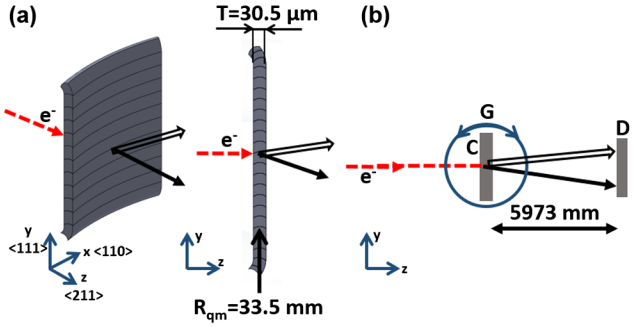

FIG. 1 (color online). (a) Bending of a silicon platelike crystal with properly chosen crystallographic orientations generates the quasimosaic effect, resulting in a secondary bending of the planes lying in the crystal thickness. (b) Sketch of the experimental setup. The dashed arrow indicates the incoming beam, impinging on the crystal mounted on a high-precision goniometer (G). The solid-black arrow indicates particles deflected thanks to planar channeling, while solid-white arrow correspond to overbarrier particles. A silicon detector, (D), reconstructs the beam profile after interaction with the crystal.

"dicing before grinding" process [33], typically used in silicon micromachining. In order to achieve the desired bending, the crystal was bent by means of a mechanical holder. The crystal was characterized by high-resolution x-ray diffraction (Panalytical X-Pert MRD-PRO), highlighting a bending angle of 905 ± 15 μrad for the (111) planes, corresponding to a radius of 33.5 mm, i.e., 23 times the critical radius [see Fig. 1(a)]. The crystal lateral sizes were optimized to suppress parasitic anticlastic deformation across the central region of the crystal [31,34] resulting in a cylindrical surface. The experimental setup is sketched in Fig. 1.

The crystal holder was mounted on a high-precision goniometer equipped with 5 degrees of freedom. Translations along the x and y axes were used to geometrically align the crystal with the beam with an accuracy of 1 μm, while rotations around the x, y and z axes with an accuracy of 50, 9, and 175 μrad, respectively, were used to achieve angular alignment of the crystal planes with the electron beam. A 855 MeV electron beam, available at the MAinz MIctrotron (MAMI) facility, was conditioned to a beam size of 200×70 μm^2 and a divergence of 70 and 30 μrad along the horizontal and vertical directions, respectively, i.e., much less than the planar critical angle, 217 μrad at 855 MeV. A unit of the "INSULAB Telescope" [35] has been used to reconstruct the beam profile after the interaction with the crystal. The detector was placed 5973 mm downstream of the crystal, allowing a spatial resolution better than 10 μm [35]. The entire experimental setup was kept under vacuum to avoid multiple scattering of the beam by air.

In order to excite coherent interactions between electrons and the crystal, the latter was rotated around the x axis and, for each angular position, the particle distribution after interaction with the crystal was recorded. A peculiarity of this experimental scheme is the separate observation of channeled and dechanneled particles, which could not be afforded by operating with a straight crystal.

The particle distribution after interaction with the crystal as a function of the crystal-beam angle is shown in Fig. 2.

This pattern very much resembles the results of the interaction between a bent crystal and π^- carried out at an energy more than 2 orders of magnitude higher [26]. Figure 2 also highlights that the same phenomena were observed either at 150 GeV or 855 MeV. In particular, in regions (1) and (6), the beam trajectory is never tangent to the crystalline planes so that coherent interactions are prevented. In region (2), the crystal is oriented for channeling, which arises as the beam impinges onto the crystal planes at an angle less than the critical angle for channeling (217 μrad) [3]. Under such conditions, the particle's transverse motion is governed by the interatomic potential averaged along the crystal planes [3,36]. However, due to multiple scattering, channeled electrons may be subject

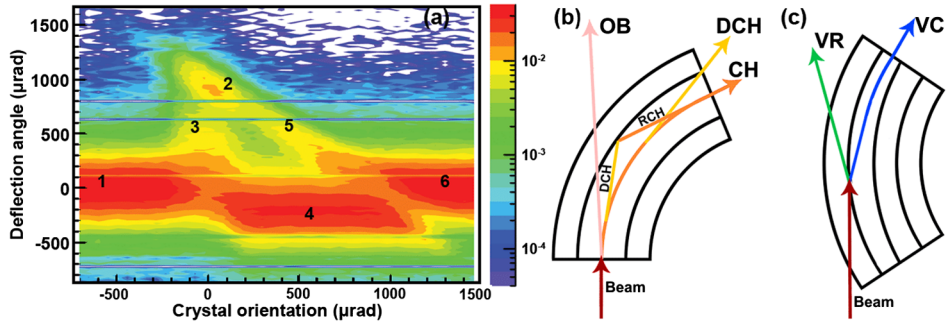

FIG. 2 (color online). (a) An "angular scan" recorded during the interaction between the crystal and the electron beam. Six different regions can be distinguished: (1) and (6) nonchanneling, (2) channeling, (3) dechanneling, (4) volume reflection, and (5) volume capture. (b) The bent crystal is aligned with respect to the charged particle beam to excite planar channeling. Overbarrier particles are deflected toward the opposite side as that of crystal bending. Underbarrier particles are captured under the channeling regime (CH). Because of multiple scattering, channeled particles may suffer dechanneling (DCH). A fraction of dechanneled particles experiences rechanneling (RCH). (c) Bent crystal is aligned with respect to the incoming particle beam (red-dashed arrow) in such a way that the beam trajectory becomes tangent to the atomic planes inside the crystal. Under such regime, either VR or the competitive process of VC occurs.

to an increase in their transverse energy and overcome the interplanar potential barrier, resulting in the dechanneling [region (3)]. The inverse of such a process may occur, too; i.e., a nonchanneled electron loses part of its transverse energy due to multiple scattering and gets trapped in the channeling mode. This effect is referred to as rechanneling, which will be shown to play a fundamental role for efficient deflection.

Aside from channeling, VR and volume capture (VC) [regions (4) and (5), respectively] manifest themselves as the trajectory of the beam becomes tangent to the bent atomic planes inside the volume of the crystal [see Fig. 2(c)]. Particles subject to VR are "reflected" by the atomic planes, being deflected to the opposite side as that of crystal bending. In contrast, particles subject to VC are captured into the channeling regime inside the crystal volume. VC occurs in the proximity of atomic planes, which correspond to the positions of maxima and minima of the interplanar potential for positive and negative particles, respectively. Thereby, due to a wealth of possible final states for negative particles, these latter are more likely to lose a larger amount of energy than the positive ones; i.e., they are easier to be captured into channeling states through VC.

Both VR and VC have an angular acceptance equal to the crystal bending angle, unlike channeling, in which the angular acceptance is limited by the critical angle.

Figure 3 shows beam profiles under either channeling or VR alignment (black curves) as compared with the predictions of Monte Carlo simulations (red curves). The code uses an inter-planar potential based on measured atomic form factors for Si [37] and solves the equation of motion for the electrons interacting with the crystal. The code does not take into account radiative losses since they are negligible because the crystal length is 3×10^{-4} times the radiation length. More information about the code can be found in Ref. [38], and references therein.

In Fig. 3, the right peak of blue curve corresponds to the particles deflected under channeling. A Gaussian fit of the distribution highlights a deflection angle of 910 ± 5 μrad. The fraction of deflected particles within $\pm 3\sigma$ around the channeling peak was $20.1 \pm 1.2\%$, a value in agreement with the simulation results (21.2%). The left peak of the blue curve is due to deflection of overbarrier particles [7], whose distribution is centered to the opposite direction

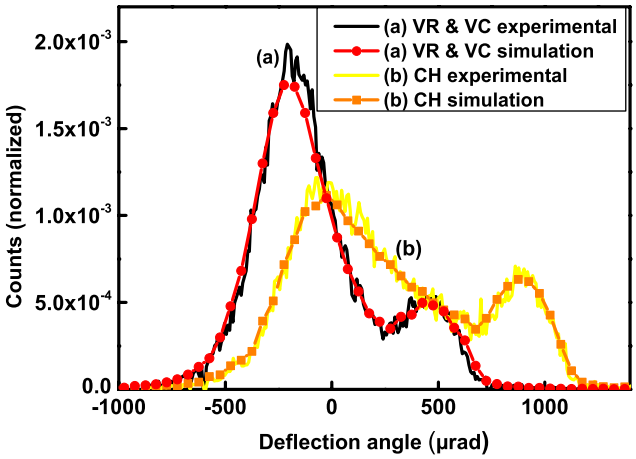

FIG. 3 (color online). (a) Beam profile with the crystal aligned for VR and VC: solid line for experimental and dash line with dots for simulation. A largest fraction of the beam is steered toward the direction opposite of channeling (left peak). VR efficiency is limited by VC (smaller right peak), deflecting particles along the crystal bending. (b) Beam profile with the crystal aligned for channeling (solid line experimental, line with squares simulation). A large fraction of the beam is deflected to the nominal deflection of the crystal (right peak). Particles found in over barrier states at the crystal entry face populate the left peak in the distribution, while the region between the two peaks is populated by particles suffering dechanneling.

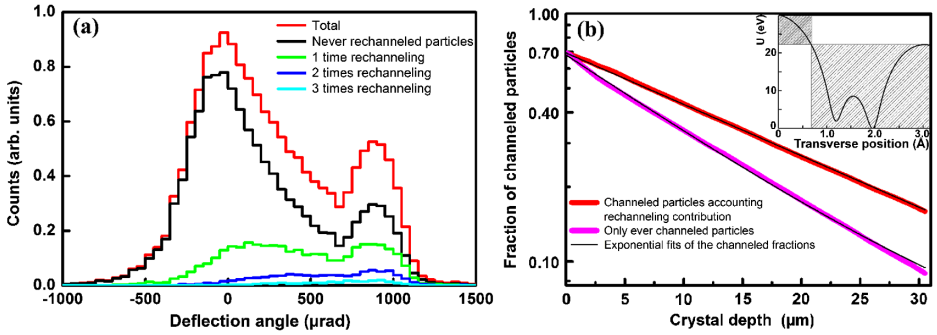

FIG. 4 (color online). (a) Monte Carlo simulation of the contributions to the angular distribution originated from rechanneled particles. The red line represents the whole distribution; black line the particles that have never been rechanneled; green, blue, and light blue lines the distribution of the particles rechanneled 1, 2, and 3 times, respectively. (b) The red curve represents the fraction of channeled particles summing up the contribution of never dechanneled particles and rechanneled particles. The magenta curve represents the fraction of never dechanneled particles. Because of crystal bending the fraction of channeled particles at the crystal entry face is not equal to unity because the centrifugal force renders asymmetric the potential, and some of the particles (impact parameter between 0 and ~0.6 Å) are not channeled (see the inset).

as that of channeling. The distribution is asymmetric because of the contribution of rapidly dechanneled particles on the right side. Following the approach described in Refs. [4,24], the beam profile recorded for channeling was fitted as the sum of two Gaussians and one exponential curve. The decay constant of the exponential term provides a direct experimental measurement of the dechanneling length, which results to be 19.2 ± 1.5 μm.

The black curve in Fig. 3 shows the deflection occurring as the crystal is oriented on the middle of the VR region (450 μrad far from the channeling peak). A Gaussian fit to the reflected beam distribution yields a deflection angle of -191 ± 10 μrad with an efficiency of $76.7 \pm 1.1\%$, in agreement with the prediction of the Monte Carlo simulation (75.8%). As expected, VR occurs with lower efficiency with respect to higher-energy experiments [8,26], because of a larger probability of competitive VC at lower energies, discussed for positively charged particles in [39]. In fact, VC is aided by incoherent scattering, which favors the transition from overbarrier to channeling states, and that becomes stronger at lower energies [38], especially for negatively charged particles.

Monte Carlo simulation allows the reproduction of observed angular distributions and also permits an insight into the particle dynamics, which could not be directly inferred from experimental data. For example, Fig. 4(a) illustrates the contributions of both single and multiple rechannelings to build up the "channeling peak" shown in Figs. 2(a) and 3(a), whereas Fig. 4(b) shows the fraction of channeled particles with and without taking into account the fraction of rechanneled electrons. Analysis of Monte Carlo simulation shows that about 55% of the particles recorded under the "channeling peak" has been recycled once at least through rechanneling.

Analysis of simulation output shows that the length causing an e fold of the fraction of channeled particles [Fig. 4(b)] (dechanneling length) for permanently channeled electrons is $L_n' = 13.6$ μm (magenta line); it becomes $L_n = 19.5$ μm if the total fraction of channeled particles, including the rechanneled ones is considered (red line). The latter value is in good agreement with the experimentally measured one. Simulation allows estimating the fraction of channeled particles at the crystal exit as 16% if rechanneling is taken into account and as 9% if not. Monte Carlo simulations were carried out in order to determine the influence of the crystal curvature on the dechanneling length with (L_n) and without (L_n') rechanneling [40] (see Table I). Rechanneling plays a significant role for moderate curvatures.

This strong contribution of rechanneling to particle dynamics is a peculiarity of channeling with negatively charged particles. Indeed, recent simulations of electron beam dynamics in straight crystals and in crystals with a periodical deformation have demonstrated the essential importance of electron rechanneling in the GeV energy range [38,41,42]. An indirect experimental evidence of the role of rechanneling was revealed in the radiation-loss spectrum of 150 GeV electrons axially channeled in a germanium crystal, building up the "Belkacem peak" [43].

TABLE I. Dechanneling lengths of 855 MeV electrons channeled between (111) planes of a silicon crystal as a function of the crystal bending radius (left column). L_n values accounting for rechanneling, while L_n' values are obtained neglecting the rechanneling contribution.

Bending radius (mm)	L_n (μm)	L_n' (μm)
8	6.9	4.9
16	13.6	10.2
33	19.5	13.6
67	25.5	15.4
134	35.5	16.2
Flat	47.2	16.5

TABLE II. Collection of all the experimentally measured L_n, values for negative particles under experimental conditions nowadays explored.

Plane	Particle and energy	L_n, yes RCH (mm)	Comment
(111)	e^-855 MeV	0.0203	Crystal bent at a radius $R = 33.5$ mm (this work)
(111)	π^-150 GeV	~0.9	Crystal bent at a radius $R = 12.92$ m [26]
(110)	e^-855 MeV	0.018	Straight crystal [30]
(110)	π^-150 GeV	0.93	Crystal bent at a radius $R = 19.2$ m [24]

Simulations [44] demonstrated that rechanneling was partly responsible for radiation amplification. Still in the axial case, the mechanism of rechanneling [45,46] was used for the interpretation of deflection of 150 GeV/c negative pions in a Si bent crystal [27]. However, lack of experimental data for rechanneling in the planar case has prevented any comparison with theories.

For the more investigated case of positively charged particles, rechanneling does not significantly impact the particle's dynamics. Indeed, two dechanneling mechanisms coexist, i.e., nuclear and electronic dechannelings. Once particles have just entered the crystal in a channeling state, those particles impinging close to the atomic planes (about 23% [4]) are rapidly dechanneled because of the incoherent interaction with inner shell electrons and atomic nuclei (nuclear dechanneling). The remaining particles (about 77%) moving far from atomic planes are subject to interaction with valence electrons only. For such particles electron dechanneling occurs as a slow process [4]. Since rechanneling occurs for dechanneled particles, the relatively small proportion of dechanneled and fast dechanneling of rechanneled particles do not render rechanneling as a relevant effect for positive particles. Conversely, negatively charged particles are mostly subject to fast nuclear dechanneling because their trajectories always intersect atomic planes so that pure electronic dechanneling is prevented [24]. Indeed, in Ref. [24] it was shown that, under peer conditions, the dechanneling length for negative particles is of the same order of the nuclear dechanneling length for positive particles, i.e., far shorter than the electronic dechanneling length for such particles. Since rechanneling is mainly fed by nuclear dechanneling, the stronger the latter the more intense the former. Moreover, as previously highlighted, the probability of capture of overbarrier particles into channeling states is larger for the case of negative particles than for the positive ones. Thus, the combined effect of stronger dechanneling and more probable VC makes rechanneling still more effective for negative particles than for their positive counterpart.

With the aim to provide state-of-the-art information on the dechanneling length of negative particle beams, we report in Table II a summary of recorded values, which were taken under different experimental conditions.

In summary, the dynamics of sub-GeV electrons in a short and bent (111) oriented Si crystal has been studied through experimental work. Planar channeling and volume reflection proved to be effective for efficient steering of the particle beam. Monte Carlo simulations of particle dynamics allows complete interpretation of experimental records and highlights the key role played by rechanneling. Rechanneling makes the effective dechanneling length to be longer than the level foreseen with no rechanneling. Such information is important for the dynamics of sub-GeV electrons subject to coherent interactions with bent crystals. As an example, it must be taken into account to simulate and design periodically bent crystals as innovative sources of high-intensity electromagnetic radiation. As another, rechanneling alters the electron's dynamics and in turn the electromagnetic radiation generated as a result of coherent interaction, thereby upcoming experiments operating with sub-GeV or GeV electron beams, i.e., FACET [47] or ESTB [48] should also take into account this effect.

This work has been funded by the ICE-RAD INFN project, by the Deutsche Forschungsgemeinschaft DFG under contract BA 1336/2-1 and by the European Commission IRSES CUTE 269131 project (Crystalline Undulator: Theory and Experiment). In particular, we acknowledge Professor A. V. Solovyov and Professor A. V. Korol for useful discussions on the subject of this work, Dr. Gerald Klug and Dr. Eugen Eurich from Disco Europe (Munich, Germany) for their support in crystal manufacturing, Mr. Persiani Andrea and Mr. Manfredi Claudio of Perman (Loiano, Italy) for their support with crystal holders manufacturing. Gilles Frequet from Fogale Nanotech for precise measurement of crystal thickness by means of a T-MAP IR interferometer.

*Corresponding author.
guidi@fe.infn.it

[1] E. N. Tsyganov, Fermilab TM-682 (1976).
[2] V. M. Biryukov, Y. A. Chesnokov, V. I. Kotov, and V. M. Biryukov, *Crystal Channeling and Its Application at High-Energy Accelerators* (Springer-Verlag Berin and Heidelberg GmbH & Co. K, 2010).
[3] J. Lindhard, Kongelige Danske Videnskabernes Selskab **34**, 14 (1965).
[4] W. Scandale *et al.*, Phys. Lett. B **680**, 129 (2009).
[5] S. P. Moller, E. Uggerhøj, H. W. Atherton, M. Clément, N. Doble, K. Elsener, L. Gatignon, P. Grafström, M. Hage-Ali, and P. Siffert, Phys. Lett. B **256**, 91 (1991).

[6] W. Scandale *et al.*, Phys. Rev. Lett. **101**, 164801 (2008).
[7] A. M. Taratin and S. A. Vorobiev, Nucl. Instrum. Methods Phys. Res., Sect. B **26**, 512 (1987).
[8] W. Scandale *et al.*, Phys. Rev. Lett. **98**, 154801 (2007).
[9] V. Guidi, A. Mazzolari, D. D. Salvador, and L. Bacci, Phys. Rev. Lett. **108**, (2012).
[10] W. Scandale *et al.*, Phys. Lett. B **692**, 78 (2010).
[11] W. Scandale *et al.*, Phys. Lett. B **714**, 231 (2012).
[12] D. Still *et al.* in *Proceedings of 3rd International Particle Accelerator Conference, New Orleans, LA, USA, 2012*, C1205201, MOPPD082 (2012).
[13] R. A. Carrigan *et al.*, Phys. Rev. ST Accel. Beams **5**, 043501 (2002).
[14] C. T. Murphy *et al.*, Nucl. Instrum. Methods Phys. Res., Sect. B **119**, 231 (1996).
[15] W. Scandale, Proc. SPIE Int. Soc. Opt. Eng. **6634**, 66340F (2007).
[16] S. J. Brodsky, F. Fleuret, C. Hadjidakis, and J. P. Lansberg, Phys. Rep. **522**, 239 (2013).
[17] E. Uggerhoj and U. I. Uggerhoi, Nucl. Instrum. Methods Phys. Res., Sect. B **234**, 31 (2005).
[18] V. B. S. Strokov, Y. Chesnokov, I. Endo, M. Iinuma, H. Kuroiwa, T. Ohnishi, H. Sato, S. Sawada, T. Takahashi, and K. Ueda, J. Phys. Soc. Jpn. **76**, 064007 (2007).
[19] V. G. Baryshevsky, I. Y. Dubovskaya, and A. O. Grubich, Phys. Lett. **77A**, 61 (1980).
[20] M. Tabrizi, A. V. Korol, A. V. Solov'yov, and W. Greiner, Phys. Rev. Lett. **98** (2007).
[21] A. Kostyuk, Phys. Rev. Lett. **110**, 115503 (2013).
[22] Y. N. Adishchev, P. S. Ananyin, A. N. Didenko, B. N. Kalinin, V. V. Kaplin, E. I. Rozum, A. P. Potylitsyn, S. A. Vorobiev, and V. N. Zabaev, Phys. Lett. **77A**, 263 (1980).
[23] A. Baurichter *et al.*, Nucl. Instrum. Methods Phys. Res., Sect. B **119**, 172 (1996).
[24] W. Scandale *et al.*, Phys. Lett. B **719**, 70 (2013).
[25] W. Scandale *et al.*, Europhys. Lett. **93**, 56002 (2011).
[26] W. Scandale *et al.*, Phys. Lett. B **681**, 233 (2009).
[27] W. Scandale *et al.*, Phys. Lett. B **680**, 301 (2009).
[28] W. Scandale *et al.*, Phys. Lett. B **682**, 274 (2009).
[29] D. I. Adejshvilia, G. L. Bocheka, V. I. Vit'koa, G. D. Kovalenkoa, and B. I. Shramenkoa, Radiat. Eff. Lett. **87**, 135 (1985).
[30] H. Backe, P. Kunz, W. Lauth, and A. Rueda, Nucl. Instrum. Methods Phys. Res., Sect. B **266**, 3835 (2008).
[31] V. Guidi, A. Mazzolari, D. De Salvador, and A. Carnera, J. Phys. D **42**, 182005 (2009).
[32] Y. M. Ivanov, A. A. Petrunin, and V. V. Skorobogatov, JETP Lett. **81**, 99 (2005).
[33] http://www.disco.co.jp/eg/solution/library/dbg.html.
[34] G. F. C. Searle, *Experimental Elasticity* (Cambridge University Press, Cambridge, England, 1920), p. 38.
[35] A. Berra, D. Lietti, M. Prest, and E. Vallazza, Nucl. Instrum. Methods Phys. Res., Sect. A **729**, 527 (2013).
[36] D. S. Gemmell, Rev. Mod. Phys. **46**, 129 (1974).
[37] M. Tobiyama *et al.*, Phys. Rev. B **44**, 9248 (1991).
[38] V. G. Baryshevsky and V. V. Tikhomirov, Nucl. Instrum. Methods Phys. Res., Sect. B **309**, 30 (2013).
[39] V. Biryukov, Phys. Lett. A **205**, 340 (1995).
[40] R. A. Carrigan, arXiv:1002.0359.
[41] A. Kostyuk, A. Korol, A. Solov'yov, and W. Greiner, J. Phys. B **44**, 075208 (2011).
[42] G. B. Sushko, V. G. Bezchastnov, I. A. Solov'yov, A. V. Korol, W. Greiner, and A. V. Solov'yov, J. Comput. Phys. **252**, 404 (2013).
[43] A. Belkacem *et al.*, Phys. Lett. B **177**, 211 (1986).
[44] V. V. Tikhomirov, Nucl. Instrum. Methods Phys. Res., Sect. B **36**, 282 (1989).
[45] A. M. Taratin and S. A. Vorobev, Phys. Status Solidi B **124**, 641 (1984).
[46] A. M. Taratin and S. A. Vorobiev, Phys. Lett. A **115**, 401 (1986).
[47] https://portal.slac.stanford.edu/sites/ard_public/facet/Pages/default.aspx.
[48] https://portal.slac.stanford.edu/sites/ard_public/estb/Pages/default.aspx.